

# The tight focusing of laser radiation using 4-sector polarization converter

S S Stafeev<sup>1,2</sup>, A G Nalimov<sup>1,2</sup>, L O'Faolain<sup>3</sup> and V V Kotlyar<sup>1,2</sup>

<sup>1</sup>Image Processing Systems Institute, Samara, Russia

<sup>2</sup>Samara State Aerospace University, Samara, Russia

<sup>3</sup>School of Physics and Astronomy of the University of St. Andrews, Scotland

E-mail: sergey.stafeev@gmail.com

**Abstract.** A laser beam with mixed linear-radial polarization formed by reflection of a linearly polarized light from a 4-sector micropolarizer was focused using a binary zone plate in a focal spot with diameters  $0.35 \pm 0.02$  and  $0.38 \pm 0.02$  of a wavelength.

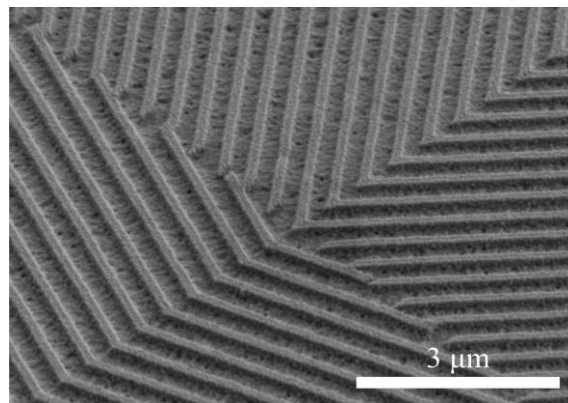
## 1. Introduction

Using of subwavelength gratings for the manipulation of polarization state of laser light was proposed for the first time in [1]. When a linearly polarized light is incident on this grating the polarization is rotated by an angle that depends from an angle between the direction of polarization of the incident light and the direction of a grating relief. In [2-4] transmitted subwavelength gratings were used to transform polarization of infrared light. However the manufacturing of these gratings for the visible region is difficult due to the high aspect ratio. Therefore previously [5] we proposed a reflected 4-sector grating polarizer for a conversion of a linearly-polarized laser beam to a radially polarized one. In this paper we have focused laser light with mixed linear-radial polarization formed by reflection of a linearly polarized light with wavelength 633 nm from a 4-sector polarization converter in a focal spot with diameters  $0.35 \pm 0.02$  and  $0.38 \pm 0.02$  of a wavelength using a binary Fresnel zone plate with focal length 532 nm.

## 2. Manufacturing

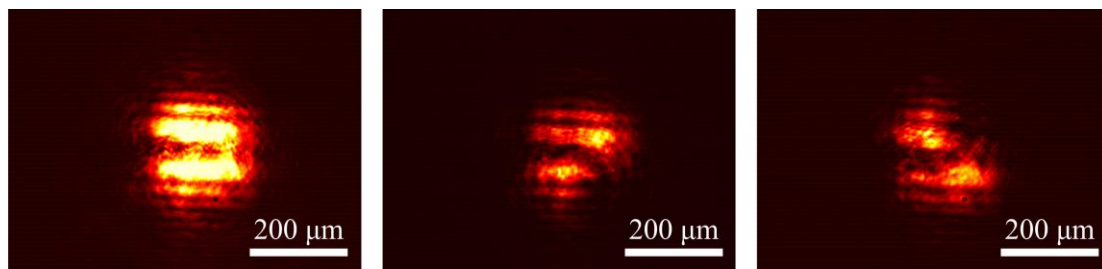
In the first step of the manufacturing a gold layer of thickness 160-180-nm was deposited on a glass substrate by electron beam evaporation. Then, the gold layer was coated with a layer of electron beam resist (ZEON ZEP520A), and the pattern of the four-sector grating polarizer projected into the resist using a 30-KV electron beam. The sample was then developed in xylene to dissolve resist fragments that had been exposed to the electron beam. The pattern of the grating polarizer was then transferred into the gold layer by sputtering with an Argon plasma. In the final stage, the remaining resist was removed with an oxygen plasma, resulting in a grating polarizer pattern engraved in gold. The duration of the reactive ion etching process was optimized so as to achieve the etch depth of the gold of about 110 nm. Figure 1 shows a SEM image of the manufactured polarizer.





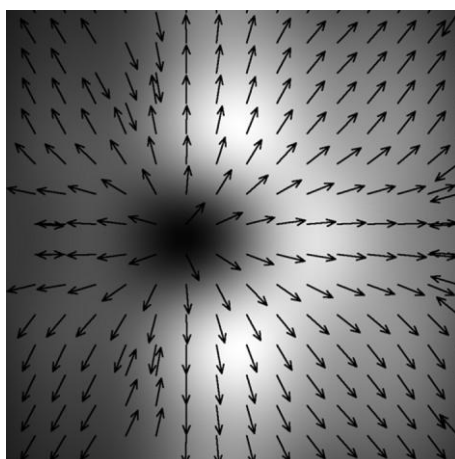
**Figure 1.** SEM image of the 4-sector polarization converter.

If a linearly polarized light reflects from the polarizer (Figure 1), the polarization is rotated by angle  $+45$  or  $-45$  relatively to direction of the incident polarization. The light reflected from the polarizer is not completely radially polarized, but is a mix of linearly polarized light and radially polarized light (in a similar way to [6]). Therefore in far field the reflected beam had a shape of a square (Figure 2a). Figures 2b and 2c show the intensity distribution in far field when an output polarizer is placed on a trajectory of the beam. Figure 2b shows the intensity of the beam when the polarizer axis is rotated by  $45^\circ$  and figure 2c shows the intensity when the polarizer axis is rotated by  $-45^\circ$ .



**Figure 2.** Far-field intensity pattern of the laser light reflected from 4-sector polarization converter: (a) without an output polarizer, with a polarizer rotated by (b)  $45^\circ$  and (c)  $-45^\circ$

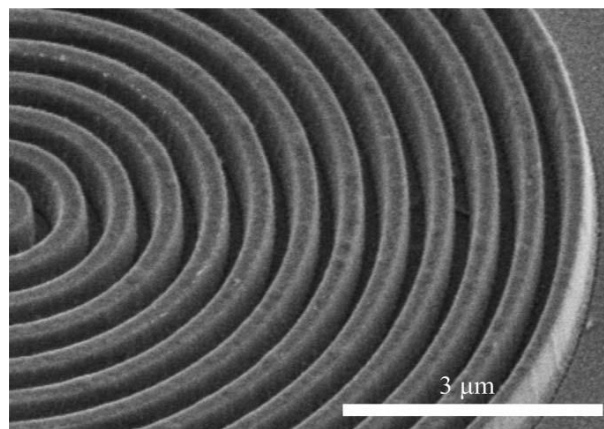
In addition previously [5] we shown that the intensity of light reflected from different sectors is not equal to each other. Figure 3 shows the calculated intensity of the light reflected from the polarizer (Figure1) at the distance  $200 \mu\text{m}$ ; the arrows depict the direction of polarization.



**Figure 3.** Intensity pattern of the light reflected from 4-sector polarizer at the distance  $200 \mu\text{m}$  from the surface. The frame size is  $5 \times 5 \mu\text{m}$ . Arrows depict the direction of the polarization.

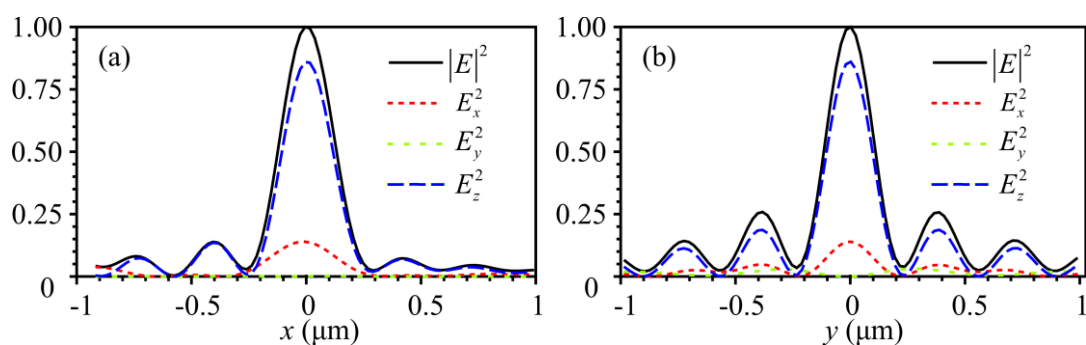
### 3. Simulation

Fresnel zone plate was used as a focusing object. The zone plate had a focal length 532 nm and was manufactured from ZEP520A resist (refractive index is equal to  $n = 1.52$ ) using ion etching. The zone plate had the following parameters: focal length 532 nm, relief depth 510 nm, diameter 14  $\mu\text{m}$ , the width of the last zone 266 nm. It should be noted that the radiuses of the zone plate were calculated for the wavelength equal to 532 nm, but in our research we illuminated the zone plate by the laser light with wavelength 633 nm. Previously [7] we shown that the zone plate illuminated by a linearly polarized Gaussian beam with wavelength 633 nm and radius 7  $\mu\text{m}$  had a focal length less than the expected focal length (230 nm). Also the experimentally obtained diameters of the focal point were equal to  $\text{FWHM}_{\min} = (0,40 \pm 0,02)\lambda$ ,  $\text{FWHM}_{\max} = (0,60 \pm 0,02)\lambda$  [7]. Figure 4 shows a SEM image of the zone plate.



**Figure 4.** SEM image of the Fresnel zone plate.

Figure 5 shows the intensity profiles in the focal spot of the zone plate in Figure 4, which is illuminated by a mixed linearly and radially polarized beam (Figure 3) from the micropolarizer in Figure 1.



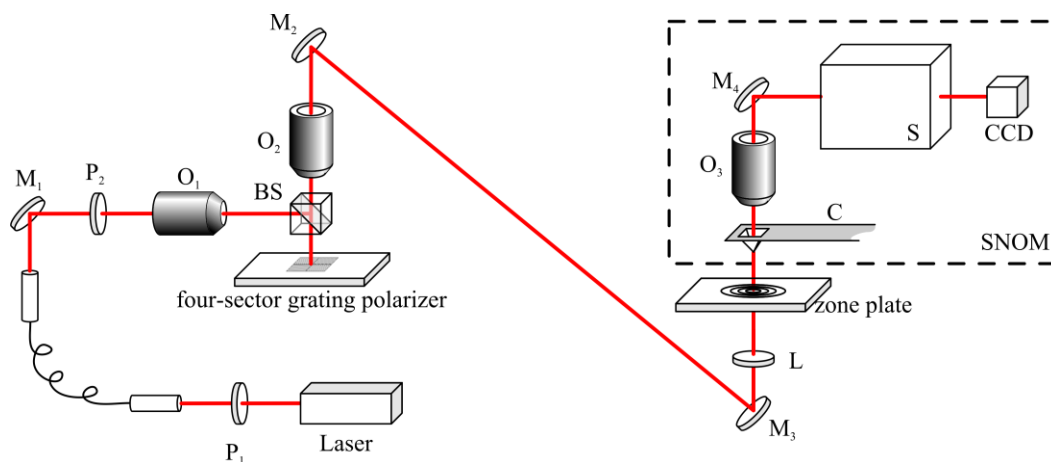
**Figure 5.** FDTD calculated intensity pattern in the focal plane of the zone plate. Sections along  $x$  axis (a) and  $y$  axis (b)

Figure 5 shows that distribution of intensity components differs from intensity distribution in a focal spot formed by linearly or radially polarized light. From Figure 5 the distribution of transverse intensity components is similar to distribution of intensity components in a focal point formed by a linearly polarized light. However distribution of longitudinal components is similar to distribution of intensity components of a radially polarized light. This has prompted us to define the beam under study as having a mixed, linear-radial polarization. In this case, instead of being a perfect circle (as in

the case of the perfect radial polarization), the focal spot is elliptical with the axial dimensions  $\text{FWHM}_{\text{max}} = (0.40 \pm 0.02)\lambda$  (Fig.5a) and  $\text{FWHM}_{\text{min}} = (0.35 \pm 0.02)\lambda$  (Fig.5b). Previously [7] we shown that a metal hollow pyramid cantilever used in SNOM measurements is 3-times more sensitive to the transverse than to the longitudinal electric field component. In this case, the focal spot is seen to be somewhat larger in size:  $\text{FWHM}_{\text{min}} = (0.36 \pm 0.02)\lambda$ .

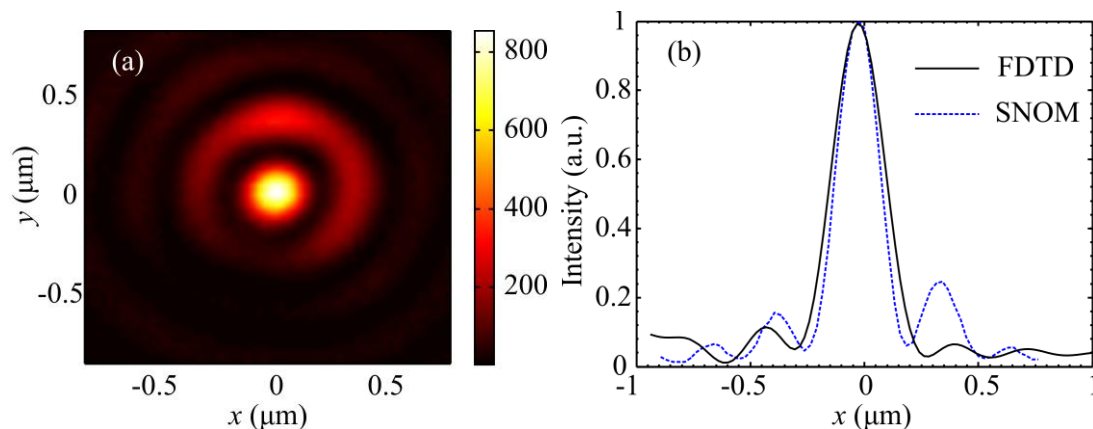
#### 4. Experiment

Figure 6 shows the experimental setup. The laser light with wavelength 633 nm was focused with an objective  $O_1$  on a 4-sector polarizer. Polarizers  $P_1$  and  $P_2$  were used to verify that the incident light is linearly polarized and to attenuate power of the incident light. Reflected from 4-sector polarizer laser light was focused on the bottom side of a substrate with the zone plate (Figure 4), propagates through the zone plate and forms a focal spot. Intensity distribution in the focal spot was measured using scanning near-field optical microscope (SNOM) Ntegra Spectra (NT-MDT). In Figure 6 SNOM is depicted as dashed rectangle.



**Figure 6.** Experimental setup. Laser, He-Ne ( $\lambda = 633$  nm);  $P_1, P_2$ : polarizers;  $M_1, M_2, M_3, M_4$ : mirrors; BS, light-splitting cube;  $O_1$ ,  $3.7\times$  objective;  $O_2$ ,  $20\times$  objective;  $O_3$ ,  $100\times$  objective; C, cantilever; L, lens; S, spectrometer; CCD, charge-coupled device camera.

Figure 7a illustrates a SNOM-aided intensity pattern, with the minimal and maximal size of the focal spot measuring  $\text{FWHM}_{\text{max}} = (0.38 \pm 0.02)\lambda$  (Fig.7b) and  $\text{FWHM}_{\text{min}} = (0.35 \pm 0.02)\lambda$  (Fig.7c). To evaluate the effect of the micropolarizer, the substrate containing the micropolarizer was shifted in the transverse direction to allow the light to be reflected at the relief-free golden surface. This resulted in a microlens-aided focal spot of dimensions  $\text{FWHM}_{\text{max}} = (0.50 \pm 0.02)\lambda$  and  $\text{FWHM}_{\text{min}} = (0.40 \pm 0.02)\lambda$ .



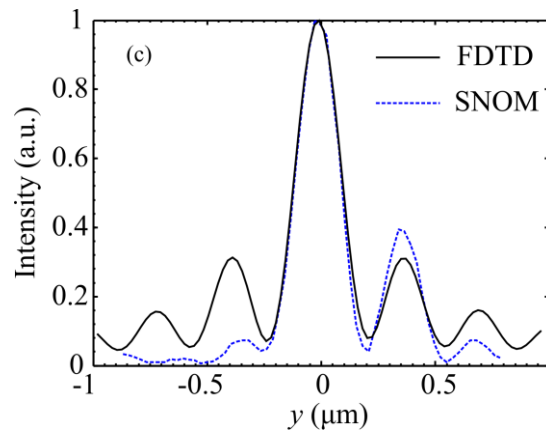


**Figure 7.** 2D Intensity pattern detected by SNOM (a) and its sections along  $x$  (b) and  $y$  axis (c).

It should be noted that recently [8] a focal spot with diameter  $0.25\lambda$  was obtained by focusing an azimuthally polarized first-order vortex beam using a conventional immersion microlens with  $NA = 1.4$ . When reduced to the common  $NA$ , the focal spot in [8] and the one reported in this work, equal to  $0.35\lambda$ , have near-same size, namely,

$$FWHM=0.25\lambda=0.25\lambda*1.4/NA=0.35\lambda/NA,$$

$$FWHM=0.35\lambda=0.35\lambda*0.997/NA=0.35\lambda/NA.$$

From the formulae above it follows that the microlens (Fig. 4) gives the same result as in [8].

## 5. Conclusion

Using a binary microlens with diameter  $14\ \mu\text{m}$  and focal length  $532\ \text{nm}$  we have focused a beam with wavelength  $633\ \text{nm}$  and mixed linear and radial polarization into a focal spot with full-width of half-maximum diameters  $(0.35\pm 0.02)\lambda$  and  $(0.38\pm 0.02)\lambda$ . The incident light was a mixture of linearly and radially polarized beams generated by reflecting a linearly polarized Gaussian beam at a gold  $100\ \mu\text{m} * 100\ \mu\text{m}$  four-sector subwavelength diffractive optical micropolarizer, with the sector gratings of period  $400\ \text{nm}$  and microrelief depth  $110\ \text{nm}$ . The focusing of a linearly polarized laser beam (other conditions being the same) has been found to produce a larger focal ellipse measuring  $(0.40\pm 0.02)\lambda$  and  $(0.50\pm 0.02)\lambda$ .

## Acknowledgements

This work was partially funded by the Ministry of Education and Science of the Russian Federation and Russian Federation Presidential grants for support of Young Candidate of Science (MK-4816.2014.2), and Russian Foundation for Basic Research grants ## 14-07-31218, 14-07-97039, 14-29-07133, 15-07-01174 and European Research Council Starting grant (no. 337508).

## References

- [1] Kotlyar V V and Zalyalov O K 1996 *Optik* **103**, 125–30.
- [2] Niv A, Biener G, Kleiner V and Hasman E 2003 *Optics Letters* **28**, 510-2.
- [3] Lerman G M and Levy U 2008 *Optics Letters* **33**, 2782-4.
- [4] Mehta A, Brown J D, Srinivasan P, Rumpf R C, Johnson E G 2007 *Optics Letters* **32**, 1935-7.
- [5] Nalimov A G, O’Faolain L, Stafeev S S, Shanina M I and Kotlyar V V 2014 *Computer Optics* **38**, 229–36.
- [6] Dorn R, Quabis S and Leuchs G 2003 *Phys. Rev. Lett.* **91** 233901.
- [7] Stafeev S, Kotlyar V and O’Faolain L 2013 *J. Mod. Opt.* **60**, 1050–9.
- [8] Li X, Venugopalan P, Ren H, Hong M and Gu M 2014 *Opt. Lett.* **39** 5961–4